Numerical Analysis of Subharmonic Mixers Using Accurate and Approximate Models

ROSS G. HICKS, STUDENT MEMBER, AND PETER J. KHAN, SENIOR MEMBER, IEEE

Abstract—**A full nonlinear numerical analysis technique is applied to subharmonically pumped mixer circuits where the two diodes are not identical. Results indicate that a slight imbalance in the diode parasitic parameters can significantly affect the mixer performance. A bilinear approximation of the Schottky-barrier diode characteristic is described, permitting accurate determination of the conversion loss peaks for millimeter-wave subharmonically pumped mixers. This approximation provides an analysis which requires significantly less computer time than a full nonlinear analysis.**

I. INTRODUCTION

IN RECENT years, there have been significant advances in the design theory of Schottky-diode mixers, associated with the removal of the restrictive assumption that the local oscillator has sinusoidal voltage or current. A variety of numerical methods [1]–[6] have been used for the nonlinear analysis of mixer circuits, with the study of Held and Kerr [7], based on the approach of Gwarek [2], being particularly significant.

Attention has also been directed to the subharmonically pumped balanced mixer, as it has several intrinsic advantages, particularly at millimeter-wave frequencies. The symmetry of the balanced mixer ensures that down-converted AM noise from the local oscillator is cancelled at the intermediate-frequency terminals. Operation with the local oscillator near half the signal frequency is cost efficient at millimeter wavelengths, where the cost of pump power increases rapidly with frequency. Kerr [8] has presented a detailed analysis of these mixers for the case where the two diodes are assumed to be identical. In practice, it has not been possible to reproduce the theoretical results readily under experimental conditions, although some encouraging experimental results have been reported [9]–[12]. Researchers have found that both slight changes in diode mounting and replacement of diodes have had a pronounced effect on performance [13].

This paper reports on the development of an accurate numerical method for the nonlinear analysis of balanced subharmonically pumped mixers, for the important practical case where the two diodes differ, either in device characteristics or in mounting configurations. In addition, the paper presents an approximate approach based on a bilinear diode model, which requires much less computational effort and yields results of sufficient accuracy for many design purposes. The bilinear model is applied to both equal-diode and unequal-diode circuits, and the results of a comparative study between the bilinear model and the nonlinear analysis method are presented.

The approach of Kerr [8] can be applied but with difficulty to the unsymmetrical subharmonically pumped mixer diode case, since in its form described in [8], it relies on the circuit symmetry to reduce the multidiode circuit to an equivalent single-diode circuit which may be readily analyzed by the techniques available in the literature. A generalization of the Kerr multiple reflection algorithm [4] to the general multidiode situation has been reported recently by Faber and Gwarek [14]. This method has not been used here as performance figures [5] based on the single-diode counterparts of the two-diode analysis methods available indicate the method described here has significant advantages of efficiency over the Faber and Gwarek approach.

Although the numerical approach described in this paper is efficient, it shares with the approaches of Kerr [8] and Faber and Gwarek [14] the requirement of substantial amounts of computer time for the following reasons: 1) the large number of calculations involved in the numerical integration of the nonlinear differential equations representing the junction varactor capacitance and the Schottky-barrier junction; and 2) the number of iterations required to ensure the linear embedding circuit constraints at the pump frequency and its harmonics are satisfied.

Because of the computational effort required for this nonlinear analysis, attention has also been directed to the accuracy attainable using simplified bilinear diode models. Barber [15] first proposed such a model for the single-diode mixer, with the mixer properties being chiefly determined by the pulse duty ratio of the switch. Bordonskiy *et al.* [16] expanded on Barber's switch model by extending the number of sidebands under consideration together with making an allowance for broad-band nonzero terminating impedances at both the image and sum frequencies. Both Barber and Bordonskiy commented on the diode cutoff frequency as being a parameter of fundamental importance in that it sets the upper frequency limit of performance for the parallel *RC* junction device. Zabyshnyi *et al.* [17] extended the work of Bordonskiy to the case of subharmonic mixers, using the assumption of identical diodes. However, the

Manuscript received March 16, 1982; revised June 9, 1982. This work was supported in part by United States ARO Grant DAA G29-76-G-0279, the Australian Research Grants Committee Grant F76/15147, and the Radio Research Board.

The authors are with the Department of Electrical Engineering, University of Queensland, St. Lucia, Queensland, 4067, Australia.

0018-9480/82/1200-2113$00.75 ©1982 IEEE

approach of Zabyshnyi fails to account for the crucial effect of the parasitic lead inductance, which at resonance induces multiple conductions in each voltage waveform [8]. The analysis, however, did emphasize the importance of the diode cutoff frequency in determining mixer performance.

II. Multidiode Update Nonlinear Analysis Approach

The approach [18] described here is based upon an extension of a single-diode nonlinear analysis technique previously published [5], [6] by the present authors. It is based upon subdivision of the circuit into three subnetworks, comprising two nonlinear one-ports and a connecting linear two-port containing the embedding network within which the pump source is located, as shown in Fig. 1.

The two-port network will be described at each harmonic of the pump frequency, using Z parameters, as follows:

$$V_1(\omega) = -Z_{11}(\omega)I_1(\omega) + Z_{12}(\omega)I_2(\omega) + V_1^{oc}(\omega) \quad (1)$$

$$-V_2(\omega) = -Z_{21}(\omega)I_1(\omega) + Z_{22}(\omega)I_2(\omega) - V_2^{oc}(\omega) \quad (2)$$

where $V_1^{oc}(\omega)$ = voltage at port 1 with both ports 1 and 2 open-circuited and represents the component due to the exciting source; $V_2^{oc}(\omega)$ = voltage at port 2 with both ports 1 and 2 open-circuited and again represents the component attributable to the exciting source. For a symmetrical reciprocal embedding network

$$Z_{12}(\omega) = Z_{21}(\omega) \quad (3)$$

$$Z_{11}(\omega) = Z_{22}(\omega) \quad (4)$$

$$V_1^{oc}(\omega) = -V_2^{oc}(\omega). \quad (5)$$

The procedure then goes as follows.

1) To commence the algorithm, sinusoidal waveforms are assumed for $I_1^o(t)$ and $V_2^o(t)$, where the superscript indicates this is the initial iteration. These values are taken at the excitation frequency, without harmonics, and may be found by an approximate calculation. Each iteration will seek to improve the values of $I_1(t)$ and $V_2(t)$.

2) The periodic voltage response $V_1^o(t)$ that diode 1 produces in response to the input $I_1^o(t)$ may be determined by successively integrating (using the classical Runge–Kutta algorithm) the nonlinear Schottky-diode equation until the transients decay, i.e.,

$$\frac{dV_1^o(t)}{dt} = \frac{I_1^o(t) - i_1\left[\exp\left(qV_1^0(t)/\eta kT\right) - 1\right]}{C_1\left(V_1^o(t)\right)} \quad (6)$$

where the capacitance term is calculated using the normal varactor equation, i.e.,

$$C_1\left(V_1(t)\right) = C_{01}\left(1 - V_1(t)/\phi\right)^{-\gamma} \quad (7)$$

where

- C_{01} zero bias capacitance for diode 1
- γ doping profile index
- ϕ contact potential
- i_1 diode 1 saturation current, and
- η diode ideality factor.

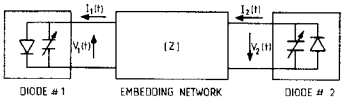

Fig. 1. Subdivision of the subharmonic mixer circuit into the two nonlinear diodes and the linear embedding network. The pump source is contained within the embedding network.

Typically, 64 points are considered in the integration computation, allowing consideration of harmonics in $V_1^o(t)$ up to the eighth order with a minimal truncation error in the Runge–Kutta algorithm.

3) Using the assumed waveforms for $I_1^o(t)$ and $V_2^o(t)$, together with the calculated waveform of $V_1^o(t)$, as given by (6), enables the fourth variable of the two-port network to be calculated. This variable, $I_2^o(t)$, the current flowing into the linear network, may be calculated using the known Z parameters of the two-port as follows:

$$I_2(\omega) = \frac{V_2(\omega) - Z_{21}(\omega)I_1(\omega) - V_2^{oc}(\omega)}{-Z_{22}(\omega)}. \quad (8)$$

The above linear embedding network calculations are most efficiently done in the frequency domain. The fast Fourier transform is used to convert between the frequency and the time domain.

4) With $I_2^o(t)$ available, a revised voltage $V_2^*(t)$ at port 2 may be calculated in the same manner as for diode 1 (revised voltages are indicated by a superscript *)

$$\frac{dV_2^*(t)}{dt} = \frac{I_2(t) - i_2\left[\exp\left(qV_2^*(t)/\eta kT\right) - 1\right]}{C_2\left(V^*(t)\right)} \quad (9)$$

where

$$C_2\left(V_2^*(t)\right) = C_{02}\left(1 - V_2^*(t)/\phi\right)^{-\gamma} \quad (10)$$

where

- C_{02} zero bias capacitance for diode 2
- γ doping profile index
- ϕ contact potential
- i_2 diode 2 saturation current, and
- η diode ideality factor.

5) Similarly, a revised $I_1^*(\omega)$ may be calculated in the frequency domain since $V_2^*(\omega)$, $I_2^o(\omega)$, and $V_1^o(\omega)$ are known quantities as is the embedding network information

$$I_1(\omega) = \frac{V_1(\omega) - Z_{12}(\omega)I_2(\omega) - V_1^{oc}(\omega)}{-Z_{11}(\omega)}. \quad (11)$$

6) It remains now to specify how the new estimates of voltage $V_2^1(t)$ and $I_1^1(t)$ are determined at the beginning of the next iteration and thereafter for each successive iteration. Two convergence parameters p_1 and p_2, one for each diode, are introduced. The range of values of these parameters is restricted to $0 < p \leqslant 1$. Values of p may be permitted to become complex [6] but experience has shown there is little advantage over using real p values. Determination of their values is based on criteria derived from a detailed convergence analysis to be given in the Appendix. These parameters are used to provide the next iteration of $I_1(t)$

and $V_2(t)$, namely $I_1^1(t)$ and $V_2^1(t)$, i.e.,

$$I_1^1(t) = p_1 I_1^*(t) + (1-p_1) I_1^o(t) \quad (12)$$

$$V_2^1(t) = p_2 V_2^*(t) + (1-p_2) V_2^o(t). \quad (13)$$

7) One iteration of the loop has now been completed, giving revised values of the periodic waveforms $I_1(t)$ and $V_2(t)$ for the next iteration cycle which begins at step 2. Iterations proceed until stationary solutions are achieved for these waveforms. The resulting computer program required 10K words of 32-bit VAX 11/780 memory.

The Appendix details the convergence mechanism of the above iteration algorithm. None of the available two-diode methods previously reported in the literature have yet provided a detailed convergence assessment to assist the user by providing prior information on the likelihood of convergence. It is clear that for the purposes of efficient automated nonlinear computation, the analysis algorithm and convergence mechanism should be thoroughly understood. The analysis in the Appendix produces a matrix for which convergence is assured if each and every element of that matrix is small. Control over the size of these matrix elements is provided by the use of the convergence parameters p_1 and p_2.

It is clear that this technique may be readily extended to the case of more than two diodes.

III. Small Signal and Noise Analysis

The small signal analysis used follows that of Kerr [8], with the mixing elements being a parallel combination of the diode varactor capacitance and Schottky-barrier conductance. The Fourier coefficients of the capacitance and conductance waveforms permit the construction of the small-signal conversion matrix for each diode. An overall mixer admittance matrix may then be formed using the two diode conversion matrices plus the diagonal matrix representing the embedding admittance network and external load admittances. This combined overall system matrix permits the calculation of the output IF impedance and the conversion loss. As eight harmonics of the local oscillator were determined by the nonlinear analysis, this permits four upper and lower sidebands to be considered in addition to the intermediate or output frequency.

The noise analysis comprises two components: the thermal noise emanating from both the diode series resistance, and the embedding network is determined using the theory of Twiss [19]; the shot noise contribution of the two diodes is calculated using Dragone's [20] noise correlation theory. Using these two components together with the superposition principle, the input noise temperature is calculated directly in an identical manner to that done by Kerr [8].

IV. Application of the Dual Diode Update Analysis

Studies were carried out on the subharmonically pumped mixer circuit examined by Kerr, given as example 1 in his paper [8]. This circuit presents a short-circuit coupling between the two diodes at frequencies above the signal

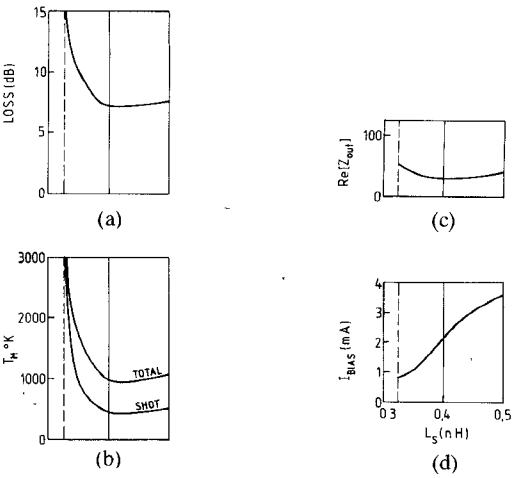

Fig. 2. The variation of mixer conversion properties with diode 2 lead inductance: (a) conversion loss, (b) input noise temperature, (c) real part of the IF-output impedance, (d) diode 2 bias current. Diode 1 parameters are: $R_s = 10\ \Omega$, $C_0 = 7.0$ fF, $L_s = 0.4$ nH, $\eta = 1.12$, $\phi = 0.95$ V, $\gamma = 0.5$, $i_0 = 8 \times 10^{-17}$ A, $i_{bias} = 2$ mA. Diode 2 parameters are identical to those of diode 1 but with the lead inductance and bias current allowed to vary.

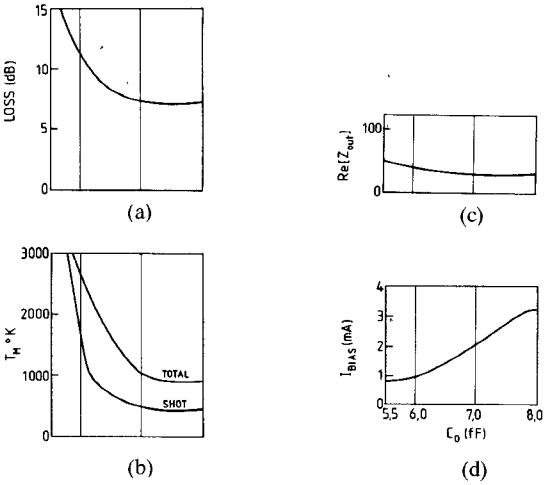

Fig. 3. The variation of mixer conversion properties with diode 2 zero-bias capacitance: (a) conversion loss, (b) input noise temperature, (c) real part of the IF-output impedance, (d) diode 2 bias current. Diode 1 parameters are identical to those given in Fig. 2. Diode 2 parameters are identical to those of diode 1 but with the zero-bias capacitance and bias current allowed to vary.

frequency. At other frequencies, the load in parallel with the diodes is 50 Ω. In the unperturbed (or equal diode case), the diode parameters used were: $R_s = 10\ \Omega$, $C_0 = 7.0$ fF, $L_s = 0.4$ nH, $\eta = 1.12$, $\phi = 0.95$ V, $\gamma = 0.5$, and $i_0 = 8 \times 10^{-17}$ A. The signal, pump, and IF are at 103, 50, and 3 GHz. The convergence parameters p_1 and p_2 were both set at 0.5 for these studies. Subsequently, both the lead inductance and zero-bias capacitance values of diode 2 were allowed to vary, yielding the effects shown in Figs. 2 and 3. In all cases, the LO power was adjusted to give a constant rectified current of 2 mA in diode 1. When the capacitance was varied, the series resistance of diode 2 was modified such that the $C_0 R_s$ product remained constant. In both Figs. 2 and 3, the rectified current of diode 2 is plotted in

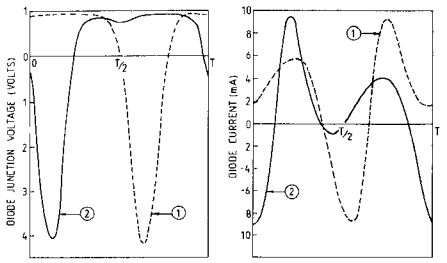

Fig. 4. Waveforms for the two diodes: (a) junction voltage, (b) diode current. Diode 2 parameters are $L_s = 0.325$ nH, $C_0 = 7.0$ fF. Diode 2 is in the resonant condition. Diode 1 parameters are $L_s = 0.4$ nH, $C_0 = 7.0$ fF.

addition to the mixer performance figures of conversion loss, input noise temperature, and IF output impedance. Typical current and voltage waveforms showing the phenomenon of double conduction [8] in diode 2 are given in Fig. 4.

It is clear from an examination of Figs. 2 and 3 that as in the identical diode situation analyzed by Kerr [8], variations in the lead inductance and zero bias capacitance in only one of the two diodes have significant effects on the overall performance of the mixer. A resonance between the lead inductance and junction capacitance of diode 2 is responsible for the poor conversion losses depicted in Figs. 2 and 3, with the resonant frequency being in the vicinity of the signal frequency. An examination of the current waveforms in Fig. 4 illustrates this point further. The resonant conditions of diode 2 are evident in the second negative current excursion; it is the increased second harmonic content which reduces the coupling of the IF current to the external IF load.

Compensation for the poor conversion losses may be achieved by addition of a separate dc bias supply for diode 2, as shown in Fig. 5. In this case, the bias voltage is adjusted until the rectified currents of both diodes (2 mA) are equal. The resulting conversion-loss diagram shows the absence of the resonant peak. In this case, the shift in the bias point on the varactor capacitance curve to a larger value of capacitance with the addition of the dc voltage tends to offset the fall in the inductance, and the resonant frequency is kept below the signal frequency.

Alternatively, when the diodes are mounted in waveguide, compensation for the variation in inductance and capacitance may be obtained readily by adjustment of the gap height. The coupled high-order TE and TM modes provide a variable reactive shunt across the gap terminals [21]. Adjustment of the gap height gives a range of compensatory reactance values for use in adjusting the diode current values for equality.

An interesting feature in both Figs. 2 and 3 is the sensitivity of the rectified current in diode 2 to the diode parameter imbalance. This has also been found experimentally, particularly in the millimeter-wave region [22]. This sharp variation in current is due to the proximity of the lead inductance-junction capacitance resonance to the fundamental pump frequency. In this situation, an increase in lead inductance tunes out a portion of the junction

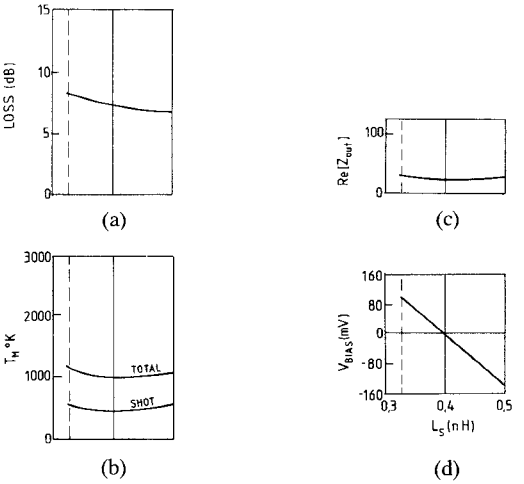

Fig. 5. The variation of mixer conversion properties with diode 2 lead inductance: (a) conversion loss, (b) input noise temperature, (c) real part of the IF output impedance, (d) diode 2 bias voltage. Diode 1 parameters are identical to those given in Fig. 2. Diode 2 parameters are identical to those of diode 1 but with lead inductance and bias voltage allowed to vary, thereby fixing the bias current of diode 2 at 2 mA.

capacitance seen at the pump frequency and thereby results in an increase in the dc-rectified current.

V. Bilinear Model

The analysis of a millimeter-wave subharmonic mixer, using a bilinear model which incorporates all the important parasitic elements, involves two steps, a large-signal analysis followed by small-signal calculations [23].

The large signal analysis is carried out using the simplified model, shown in Fig. 6, for each diode in the anti-parallel pair. In this model, C_j is taken to be the zero-bias capacitance value, and the turn-on voltage is taken to be equal to the dc bias voltage which gives rise to the required dc bias current. The pump source is assumed to be ideal and have zero internal source impedance. Two linear analyses are required for each of the two states of the switch. The switch is closed for the period during which the diode voltage across C_j is greater than or equal to $V_{\text{turn-on}}$. Clearly, at each change of the state of the bipolar switch, the two initial conditions comprising the capacitance charge together with the lead inductance flux must be determined. It is possible due to resonances and ringing to obtain multiple conductions per cycle. In this case, care must be taken to ensure this phenomenon is correctly characterized in the calculations. For each case, the conduction angle and pump voltage amplitude are required following specification of the dc bias current; in practice, a rapid iteration gives the required pump voltage value to provide the specified bias current.

The small-signal analysis involves determination of the conductance and capacitance waveforms, from which harmonic components are readily found by Fourier analysis. This analysis is carried out with the diode model shown in Fig. 7, which differs from that of Fig. 6 in provision of elements C_{j2} and R_j when diode conduction is occurring and the switch is closed. R_j is the diode conductance and the sum of C_{j1} and C_{j2} is the diode capacitance for the

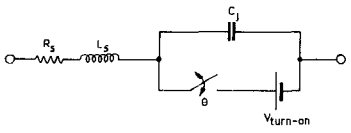

Fig. 6. Bilinear model of the mixer diode to be used in the approximate large signal nonlinear analysis. R_s is the series resistance, L_s is the lead inductance, C_j is the zero-bias capacitance, $V_{\text{turn-on}}$ is the forward bias turn-on voltage, θ is the conduction angle of the switch. Two of these diodes are connected in antiparallel to form a subharmonic mixer.

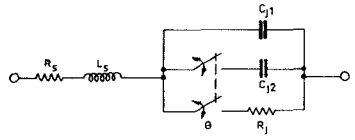

Fig. 7. Equivalent circuit of the diode used in the small signal analysis. This circuit features both a switched capacitance and a switched conductance. C_{j1} is the zero-bias capacitance, R_j is the diode conductance, and $C_{j1}+C_{j2}$ the diode capacitance for the specified dc-bias current.

specified dc bias current value; both are found using the exact diode $I-V$ and $C-V$ relations. C_{j1} now denotes the zero-bias capacitance. Using this model, together with the switch duty ratio found from the large signal bilinear model analysis, conductance and capacitance waveforms are readily found and a small-signal conversion matrix constructed for each diode.

An overall mixer admittance matrix may then be formed using the two diode conversion matrices plus the diagonal matrix representing the embedding admittance network and external load admittances. This combined overall system matrix enables calculation of the output IF impedance, conversion loss, and the input signal impedance. As in the analysis in Section III, four upper and lower sidebands were considered.

The noise analysis proceeds in two steps. Firstly, the thermal noise emanating from the diode series resistances and the embedding network is determined using the theory of Twiss [19]. The shot-noise contribution of the two diodes, each represented as an ideal switch, may be determined using the following theorem presented by Kerr [8]. A two-diode mixer, *using ideal exponential diodes* mounted in a lossless circuit, has essentially the same output noise as a lossy multiport network maintained at a temperature $\eta T/2$, where T is the physical temperature of the diodes and η is their ideality factor. From the total noise power delivered to the IF load admittance, the previously calculated conversion loss enables the input SSB noise temperature to be determined. For the switched bilinear model presented in this paper, it is assumed that the switch in the model contributes an amount of shot noise equivalent to that of the ideal exponential diode analyzed by Kerr in his theorem.

The resulting computer program required 7K words of 32-bit VAX 11/780 memory.

VI. Application of the Bilinear Model

Comparative studies were carried out on the subharmonically pumped mixer of Kerr, the circuit analyzed in Section IV using the dual-diode update nonlinear analysis.

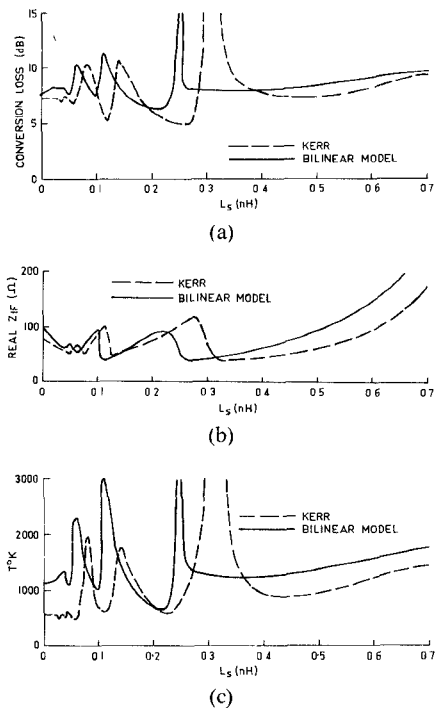

Fig. 8. Comparison of: (a) calculated conversion loss, (b) IF output impedance and (c) input noise temperature values given by the full nonlinear analysis reported by Kerr [8] and the bilinear model described in this paper. Identical diodes were used. Pump frequency = 50 GHz, signal frequency = 103 GHz, IF frequency = 3 GHz, bias current = 2 mA, $R_s = 10\ \Omega$, $C_j = 7.0$ fF.

Fig. 8 shows the variation of mixer performance with lead inductance, the diode lead inductances being constrained to be equal. The exact analysis results [8] are shown for comparison.

It is clear that the peaks given by the analysis of Kerr [8] are also predicted by the simplified bilinear model. This applies to all three properties of the mixer, namely conversion loss, IF-output impedance, and the input-signal noise temperature. However, it is equally apparent that there is a systematic horizontal displacement of the conversion peaks. Elementary LC resonance calculations using the zero-bias capacitance (based on resonance at the second pump harmonic) predict the largest conversion loss peak to occur at 0.36 nH in Fig. 8. As the average pumped capacitance is higher than the zero bias capacitance, it is to be expected that the full nonlinear analysis of Kerr [8] will shift the peak to a smaller value of inductance than 0.36 nH. The bilinear model analysis will naturally shift the peaks to a still further smaller value of inductance as the forward conduction region is effectively modelled as an infinite capacitance (short circuit), thus further increasing the average capacitance.

As may be expected, the bilinear model predicts sharper resonances than that given by Kerr [8], who used a full nonlinear analysis. This is a consequence of the absence of any diode-junction resistance in the perfect switch which was used in the diode bilinear model. On the other hand, the exponential Schottky-barrier equation inherently adds resistance to the circuit of the more comprehensive model, thereby providing damping to the LC resonant behavior of the circuit.

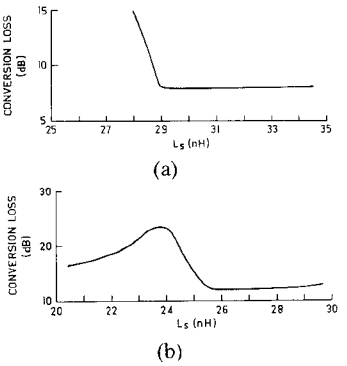

Fig. 9. Conversion loss versus diode 2 lead inductance for 2 different unequal diode situations: (a) diode 1 lead inductance = 0.30 nH, (b) diode 1 lead inductance = 0.25 nH. Other diode parameters (for both diodes) are: $R_s = 10\ \Omega$, $C_0 = 7.0$ fF. Diode 1 bias current = 2.0 mA. Note in (b) the conversion loss is always high as diode 1 is resonant at the signal frequency.

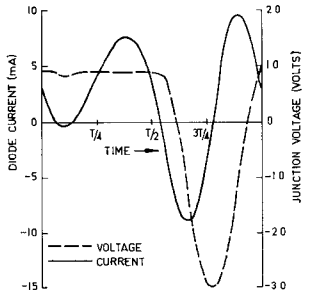

Fig. 10. Typical voltage and current waveforms calculated by the bilinear model where the phenomenon of multiple conduction is occurring. Bias current = 2 mA, $R_s = 10\ \Omega$, $C_j = 7.0$ fF, $L_s = 0.25$ nH. The two diodes are identical in this case.

The unequal diode results given in Fig. 9 reinforce the observations made in Section IV where the full nonlinear analyses were used. Diode 2 in Fig. 9(a) is in a nonresonant condition, and the subharmonic mixer performance deteriorates only when the lead inductance of diode 1 approaches 0.27 nH and the resonance at the signal frequency. On the other hand, the lead inductance of diode 2 in Fig. 9(b) is such that it produces an LC resonance at the signal frequency and thus the subharmonic mixer provides a poor response (12-dB loss) which deteriorates still further as diode 1 approaches resonant conditions. It is thus clear that, should one diode be at a resonant condition, the total mixer performance will suffer, irrespective of the condition of the other diode.

Finally, Fig. 10 depicts typical calculated voltage and current waveforms (using the bilinear model) for the case of double conduction leading to a conversion loss peak. The shape of these waveforms is virtually identical to those given in Fig. 4, which are calculated by the full update nonlinear analysis approach.

VII. Conclusions

This paper has presented a full dual-diode nonlinear analysis iteration technique whose convergence properties have been investigated. The dual-diode nonlinear analysis method requires a significant amount of computer time but enables the diodes to be fully characterized by their Schottky-barrier equations together with their nonlinear varactor capacitances. This technique has been applied to a study of a subharmonically pumped mixer with a view to establishing its performance with nonidentical diodes present. The study demonstrated the importance of the lead inductance–junction capacitance resonance which, if present in either one or both diodes, will cause a large conversion loss. This work complements the "identical diode" subharmonic mixer work reported by Kerr [8].

More rapid subharmonic mixer performance calculations may be achieved by using the bilinear model approach described in this paper. This model retains only the most significant features of the more comprehensive equivalent circuit used in the full analysis, yet still enables reasonably accurate mixer performance calculations to be made.

Appendix
Convergence Analysis

The convergence mechanism of the approach described above is investigated through a determination of the rate of error decrease per iteration cycle. Because of the two nonlinearities present, two error rates need to be monitored. Convergence to a stable solution imposes the constraint that both error magnitudes approach zero with increasing iteration number.

Let the nth harmonics of the correct solutions at the two interfaces be denoted by I_{1n}^{∞} and V_{2n}^{∞}. After m iterations

$$I_{1n}^{m} = I_{1n}^{\infty} + \delta_{1n}^{m} \tag{A1}$$

$$V_{2n}^{m} = V_{2n}^{\infty} + Z_{2n}^{NL}\delta_{2n}^{m} \tag{A2}$$

where δ_{1n}^{m} and δ_{2n}^{m} are the respective error terms, and Z_{2n}^{NL} is the impedance of diode 2 presented at the nth harmonic pump frequency.

The next iteration cycle would proceed as follows:

$$V_{1n}^{m} = Z_{1n}^{NL} I_{1n}^{m} \tag{A3}$$

where Z_{1n}^{NL} is the impedance of diode 1 presented at the nth harmonic pump frequency.

Using the embedding network information

$$I_{2n}^{m} = \left| \frac{V_{2n}^{m} - Z_{21} I_{1n}^{m} - V_{2}^{oc}}{-Z_{22}} \right|. \tag{A4}$$

The nonlinearity due to diode 2 then requires

$$V_{2n}^{*} = Z_{2n}^{NL} I_{2n}^{m}.$$

I_{1n}^{*} may then be calculated as follows:

$$I_{1n}^{*} = \left| \frac{V_{1n}^{m} - Z_{12} I_{2n}^{m} - V_{1}^{oc}}{-Z_{11}} \right|. \tag{A5}$$

The succeeding iterates, denoted with the superscript $(m+1)$, are given by

$$\begin{aligned} I_{1n}^{m+1} &= p_1 I_{1n}^{*} + (1-p_1) I_{1n}^{m} \\ &= p_1 \left| \frac{Z_{1n}^{NL} I_{1n}^{\infty} + Z_{1n}^{NL}\delta_{1n}^{m} - Z_{12} I_{2n}^{m} - V_{1}^{oc}}{-Z_{11}} \right| \\ &\quad + (1-p_1)(I_{1n}^{\infty} + \delta_{1n}^{m}) \end{aligned} \tag{A6}$$

where

$$I_{2n}^{m} = \left| \frac{V_{2n} + Z_{2n}^{NL}\delta_{2n}^{m} - Z_{21}I_{1n}^{\infty} - Z_{21}I_{1n}^{\infty} - Z_{21}\delta_{1n}^{m} - V_{2}^{oc}}{-Z_{22}} \right|. \tag{A7}$$

Using the definitions of V_{2n}^{∞} and I_{1n}^{∞}, the following simplifications can be made:

$$I_{1n}^{m+1} = I_{1n}^{\infty} + \left| p_1 \left(\frac{-Z_{1n}^{NL}Z_{22} + Z_{12}Z_{21}}{Z_{11}Z_{22}} \right) + (1-p_1) \right| \delta_{1n}^{m} + p_1 \left(\frac{-Z_{12}Z_{2n}^{NL}}{Z_{11}Z_{22}} \right) \delta_{2n}^{m} \tag{A8}$$

$$= I_{1n}^{\infty} + \delta_{1n}^{m+1} \tag{A9}$$

where δ_{1n}^{m+1} is defined by (A8) and (A9). Similarly

$$V_{2n}^{m+1} = V_{2n}^{\infty} + Z_{2n}^{NL}\delta_{2n}^{m+1} \tag{A10}$$

where

$$\delta_{2n}^{m+1} = p_2 \frac{Z_{21}}{Z_{22}} \delta_{1n}^{m} + \left| -p_2 \frac{Z_{2n}^{NL}}{Z_{22}} + (1-p_2) \right| \delta_{2n}^{m}. \tag{A11}$$

The cross coupling of the errors given by (A8)–(A11) gives rise to a matrix formulation, i.e.,

$$\boldsymbol{\delta}_{n}^{m+1} = M_n \boldsymbol{\delta}_{n}^{m} \tag{A12}$$

where

$$\text{the error vector } \boldsymbol{\delta}_{n}^{m} = \begin{pmatrix} \delta_{1n}^{m} \\ \delta_{2n}^{m} \end{pmatrix} \tag{A13}$$

and the four elements of the matrix M_n are defined by (A8)–(A11).

For convergence, a norm of M_n, denoted $\|M_n\|$, must be less than unity [24]. The norm of a matrix quantifies its magnifying power when used in vector multiplication; a small matrix norm is guaranteed by having small matrix elements. For the mixer circuits analyzed here, the lead inductances of the diodes ensure large values for Z_{11} and Z_{22}, which in turn keeps the size of the matrix elements down. In addition, the convergence parameters provide some flexibility.

References

[1] D. A. Fleri and L. D. Cohen, "Nonlinear analysis of the Schottky-barrier mixer diode," *IEEE Trans. Microwave Theory Tech.*, vol. MTT-21, pp. 39–43, Jan. 1973.

[2] W. K. Gwarek, "Nonlinear analysis of microwave mixers," M.S. thesis, Massachusetts Institute of Technology, Cambridge, MA., Sept. 1974.

[3] S. Egami, "Nonlinear, linear analysis, and computer-aided design of resistive mixer," *IEEE Trans. Microwave Theory Tech.*, vol. MTT-22, pp. 270–275, Mar. 1974.

[4] A. R. Kerr, "A technique for determining the local oscillator waveforms in a microwave mixer," *IEEE Trans. Microwave Theory Tech.*, vol. MTT-23, pp. 828–831, Oct. 1975.

[5] R. G. Hicks and P. J. Khan, "Numerical technique for determining pumped nonlinear device waveforms," *Electron. Lett.*, vol. 16, no. 10, pp. 375–376, May 8, 1980.

[6] R. G. Hicks and P. J. Khan, "Numerical analysis of nonlinear solid-state device excitation in microwave circuits," *IEEE Trans. Microwave Theory Tech.*, vol. MTT-30, pp. 251–259, Mar. 1982.

[7] D. N. Held and A. R. Kerr, "Conversion loss and noise of microwave and millimeter-wave mixers: Parts 1 and 2: Theory and experiment," *IEEE Trans. Microwave Theory Tech.*, vol. MTT-26, pp. 49–61, Feb. 1978.

[8] A. R. Kerr, "Noise and loss in balanced and subharmonically pumped mixers: Parts I and II: Theory and application," *IEEE Trans. Microwave Theory Tech.*, vol. MTT-27, pp. 938–950, Dec. 1979.

[9] T. F. McMaster, M. V. Schneider, and W. W. Snell, "Millimeter-wave receivers with subharmonic pump," *IEEE Trans. Microwave Theory Tech.*, vol. MTT-24, pp. 948–952, Dec. 1976.

[10] R. E. Forsythe, V. T. Brady, and G. T. Wrixon, "Development of a 183-GHz subharmonic mixer," in *Proc. IEEE MTT-S Int. Microwave Symp.*, (Florida), April–May 1979, pp. 20–21.

[11] E. R. Carlson, M. V. Schneider, and T. F. McMaster, "Subharmonically pumped millimeter-wave mixers," *IEEE Trans. Microwave Theory Tech.*, vol. MTT-26, pp. 706–715, Oct. 1978.

[12] M. V. Schneider and W. W. Snell, "Harmonically pumped stripline down-converter," *IEEE Trans. Microwave Theory Tech.*, vol. MTT-23, pp. 271–275, Mar. 1975.

[13] P. T. Parrish, A. G. Cardiasmenos, and I. Galin, "94-GHz beam-lead balanced mixer," *IEEE Trans. Microwave Theory Tech.*, vol. MTT-29, pp. 1150–1157, Nov. 1981.

[14] M. T. Faber and W. K. Gwarek, "Nonlinear-linear analysis of microwave mixer with any number of diodes," *IEEE Trans. Microwave Theory Tech.*, vol. MTT-28, pp. 1174–1181, Nov. 1980.

[15] M. R. Barber, "Noise figure and conversion loss of the Schottky barrier mixer diode," *IEEE Trans. Microwave Theory Tech.*, vol. MTT-15, pp. 629–635, Nov. 1967.

[16] G. S. Bordonskiy *et al.*, "Frequency converter at wavelength of 2.5 mm," *Radio Eng. Electron. Phys.*, vol. 21, no. 3, pp. 88–93, Mar. 1976.

[17] A. I. Zabyshnyi *et al.*, "Millimetre-range mixers with subharmonic pumping," *Radio Eng. Electron. Phys.*, vol. 25, no. 4, pp. 287–290, Apr. 1980.

[18] R. G. Hicks and P. J. Khan, "Analysis of balanced subharmonically pumped mixers with unsymmetrical diodes," in *Proc. IEEE MTT-S Int. Microwave Symp.*, (Los Angeles, CA), June 1981, pp. 457–459.

[19] R. Q. Twiss, "Nyquist's and Thevenin's theorems generalized for nonreciprocal linear networks," *J. Appl. Phys.*, vol. 26, no. 5, pp. 599–602, May 1955.

[20] C. Dragone, "Analysis of thermal and shot noise in pumped resistive diodes," *Bell Syst. Tech. J.*, vol. 47, pp. 1883–1902, Nov. 1968.

[21] R. L. Eisenhart, "Understanding the waveguide diode mount," in *Proc. IEEE MTT-S Int. Microwave Symp.*, (Arlington Heights), May 1972, pp. 154–156.

[22] M. Cohn, J. E. Degenford, and B. A. Newman, "Harmonic mixing with an antiparallel diode pair," *IEEE Trans. Microwave Theory Tech.*, vol. MTT-23, pp. 667–673, Aug. 1975.

[23] R. G. Hicks and P. J. Khan, "Numerical analysis of subharmonic mixers using a bilinear diode model," in *Proc. IEEE MTT-S Int. Microwave Symp.*, (Dallas, TX), June 1982, pp. 382–384.

[24] L. W. Johnson and R. D. Riess, *Numerical Analysis*. Reading: Addison–Wesley, 1977, pp. 50–61.

Ross G. Hicks (S'76) was born in Southport, Australia, on February 27, 1956. He received the B.E. (communications, with First Class Honours) degree from the University of Queensland, Brisbane, Australia, in 1976, and has since then been investigating resistive mixers as the basis of the Ph.D. degree.

His research interests also include computer circuit analysis methods, waveguide equivalent circuits, and microwave solid-state circuit design.

Mr. Hicks is a member of the Institution of Radio and Electronics Engineers, Australia, and the Institution of Engineers, Australia.

Peter J. Khan (M'61–SM'79) was born in Bowral, Australia, on November 12, 1936. He received the B.Sc. degree in mathematics and physics, and the B.E. and Ph.D. degrees in electrical engineering, all from the University of Sydney, Australia, in 1957, 1959, and 1963, respectively.

From 1953 to 1959 he was employed at the Weapons Research Establishment at Salisbury, South Australia, carrying out research and development in electronic circuits. After completion of his doctoral studies in parametric amplification, he came to the University of Michigan, Ann Arbor, MI, in 1963 with a Fulbright Post-doctoral Fellowship. He remained there until 1976, as an Assistant Professor and Associate Professor of Electrical Engineering. In 1976 he returned to Australia where he is now Reader in Electrical Engineering at the University of Queensland. His research interests include microwave solid-state circuit design, as well as fabrication and analysis of propagating structures at millimeter-wave and optical frequencies.

Aspects of the Calibration of a Single Six-Port Using a Load and Offset Reflection Standards

G. P. RIBLET, MEMBER, IEEE, AND E. R. BERTIL HANSSON

Abstract — **In this contribution some aspects of the calibration of a single six-port using a load and offset reflection standards are discussed. The applicability of the methods developed is demonstrated by the successful calibration of several six-ports including one consisting of a directional coupler plus a symmetrical five-port junction.**

I. INTRODUCTION

ALTHOUGH THE THEORY for the calibration of six-ports using the dual six-port method is well developed at this time [1], the calibration of these devices using offset reflection standards is attractive, particularly in a typical laboratory environment. Problems with the latter are a) the absence of simple closed form expressions for the calibration constants [2] and b) insight into what standards to choose to optimize the calibration over a given frequency interval. This contribution attempts to remedy this situation. A third problem of much practical significance relates to the transferability of the calibration. It is shown how the calibration constants can be normalized in such a way that a six-port can be recalibrated with a good load on the output without the need to go through a full calibration procedure whenever the device is used in a different experimental configuration.

Manuscript received March 10, 1982; revised July 2, 1982.

G. P. Riblet is with Microwave Development Laboratories, Inc., Natick, MA 01760.

E. R. Bertil Hansson was with Microwave Development Laboratories, Inc. He is now with the Division of Network Theory, Chalmers University of Technology, Gothenburg, Sweden.

II. CHOICE OF OFFSET STANDARDS

If P_R is the power measured by the reference detector and P_i, $i=1,2,3$ the powers measured by the other three detectors attached to the six-port (see Fig. 1), then the power ratios P_i/P_R can be written

$$P_i/P_R = Y^i \frac{1+2X_i|\Gamma_u|\cos(\phi_{x_i}+\phi_u)+X_i^2|\Gamma_u|^2}{1+2Z|\Gamma_u|\cos(\phi_z+\phi_u)+Z^2|\Gamma_u|^2}, \quad i=1,2,3 \quad (1)$$

where $|\Gamma_u|$ is the magnitude and ϕ_u the phase of the reflection coefficient to be measured [3]. The other quantities are calibration constants of the six-port. The term Y^i, $i=1,2,3$ can be determined from a measurement of a very good load or a sliding load on the output. If the reference coupler has infinite directivity and the six-port is perfectly matched, then Z will be zero and only terms in the numerator will appear. In general, these conditions will be approximately fulfilled so that Z will be small and the denominator will be close to one. Let us assume that Z, ϕ_z are known (a procedure is given in the next section for

0018-9480/82/1200-2120$00.75 ©1982 IEEE